Sensors & Actuators: A. Physical 337 (2022) 113441

Contents lists available at ScienceDirect

Sensors and Actuators: A. Physical

journal homepage: www.journals.elsevier.com/sensors-and-actuators-a-physical

Temperature measurement with photodiodes: Application to laser diode temperature monitoring☆

Péter Földesy [a,b,*], Imre Jánoki [a,b], Ádám Nagy [a,b], Máté Siket [a,c], Ákos Zarándy [a,b]

[a] Institute for Computer Science and Control, Budapest 1111, Hungary
[b] Faculty of Information and Bionics, Pázmány Péter Catholic University, Budapest 1083, Hungary
[c] Physiological Controls Research Center, Óbuda University, Budapest 1034, Hungary

ARTICLE INFO

Keywords:
Photodiode
Temperature measurement
Temperature control
Laser diode

ABSTRACT

The temperature feedback of solid state laser diodes and various photovoltaic devices is critical for stable and reliable usage. We demonstrate that with a simple and passive electrical measurement process and optical calibration method the temperature of a photodiode can be determined, while keeping its original purpose. We present the idea with simulation and experiments, and provide an illumination-based parameter fitting method. The presented use case is a 5.6*mm* IR laser diode. We used its monitor photodiode to track the temperature inside the package with significantly better temporal resolution than the off-the-shelf external heat sink sensor provides. We reached a time resolution in the range of milliseconds and achieved precision of ±10*mK* with ±3*K* absolute, uncalibrated precision. The technique is not restricted to laser diodes, it is applicable to photovoltaic cells, photodiode arrays, organic diodes as well.

1. Introduction

There are several pn/pin diode and bipolar junction transistor (BJT) related temperature monitoring solutions [1–4,5,6] in conjunction with temperature independent or absolute temperature proportional circuits [7]. There are several standardized techniques to measure and express the parameters of a pn/pin diode model including its temperature dependence [8–11,12]. These techniques are based on the measurement of the reverse and forward biased current-voltage characteristics. Another frequently used solution is remote temperature sensors, which monitor temperature with non-integrated silicon diodes. The common feature of these solutions is controlling the exact value or ratio of the sensing junction current to avoid device characterization [3]. This assumption is not fulfilled in the case of a photovoltaic cell or photodiode, where the external voltage-current relationship is heavily altered by the exposure-induced current flow.

We demonstrate that the absolute temperature of a photodiode can be estimated with relying only on arbitrary optical stimuli and monitoring the short circuit and open circuit voltage. The measurement is passive: there is no current explicitly forced through the diode to measure its characteristics. The feasibility of this technique is illustrated on the monitor photodiode of laser diodes. Temperature dynamics simulation and measurements of transistor outline (TO) can packaged laser diode are presented. The reason for the choice is that measuring the temperature of the diodes constantly and precisely guarantees wavelength and optical power stability [13]. Additionally, laser diodes age quickly at elevated temperature which can be addressed using feedback controlled cooling. Junction temperature monitoring may need complex optical setups [14,15] or thermal imaging [16,17]. The most common and cost effective encapsulation type of laser diodes is a flavor of metal TO package. These metal packages usually integrate a photodiode for short term power references with no guaranteed accuracy. We propose to use these photodiodes to measure the temperature of the laser chip instead. Their thermal connection to the laser diode chips is excellent and their thermal mass is very low, making them a good candidate for following laser diode temperature dynamics. The illumination independent relative precision reached is in the 10*mK* range with ± 3*K* absolute precision at millisecond timescale for a 250*mW* IR laser diode.

☆ This research was funded by the National Research, Development and Innovation Office, Hungary, grant 1019658 and the Ministry of Innovation and Technology NRDI Office, Hungary within the framework of the Artificial Intelligence National Laboratory Program.

* Corresponding author.
E-mail addresses: foldesy.peter@sztaki.hu (P. Földesy), foldesy.peter@sztaki.hu (I. Jánoki), foldesy.peter@sztaki.hu (Á. Nagy), foldesy.peter@sztaki.hu (M. Siket), foldesy.peter@sztaki.hu (Á. Zarándy).

https://doi.org/10.1016/j.sna.2022.113441
Received 29 October 2021; Received in revised form 19 January 2022; Accepted 7 February 2022
Available online 10 February 2022

2. Operation principles

The absolute temperature of a photodiode is calculated by inferring temperature from its measured electrical properties with no external electrical stimuli and regardless of its optical input. In order to do that, the open circuit voltage (V_{OC}) and the short circuit current (I_{SC}) is monitored and the diode I/V equations are solved. To identify various physical parameters of the photodiode, we propose an optical stimuli based calibration method.

2.1. Diode equations

The current flow through a p-n junction is a well understood process [18]. The junction current can be modeled by the current through barrier according to the thermionic emission (TE) theory, and can be expressed as [19–22]:

$$I = I_0 exp\left(\frac{q(V_{FB} - I_{ph}R_s)}{nkT} - 1\right) - I_{ph}, \tag{1}$$

where q is the absolute value of electron charge, V_{FB} is the forward bias voltage, I_{ph} is the current of the photodiode, R_s is the series resistance including the resistance of the contacts and the resistance of the non-depleted silicon, n is the ideality factor, k is the Boltzmann constant, and T is the absolute temperature. I_0 is the saturation current, given by

$$I_0 = AA^* T^K exp\left(-\frac{q\phi_B(T)}{nkT}\right) \tag{2}$$

where A is the rectifier contact area, A* is the Richardson constant (146 A/cm^2K^2 for n-type Si), $\phi_B(T)$ is the barrier height and K is the temperature exponent. The ideality factor n is used to take into account the deviation of the actual, manufactured diode from an ideal one. ϕ_B is also temperature dependent and can be modeled as [23]:

$$\phi_B(T) = \phi_B(0) - \frac{\alpha T^2}{T + \beta} \tag{3}$$

where the parameters are $\phi_B(0) = 1.166eV$, $\alpha = 4.73 \cdot 10^{-4} eV/K$, and $\beta = 636K$ for silicon. In the case of open circuit configuration (photovoltaic), the external current becomes zero and open circuit voltage is equal to the forward bias voltage: $V_{OC} = V_{FB}$ is measured. In zero bias case, the terminals of the photosensor are shortened ($V_{FB} = 0$) and the short circuit current is equal to the photodiode current: $I_{SC} = I_{ph}$ can be measured [21].

2.2. Parameter fitting and calibration

In order to solve the diode Eqs. (1), (2), and (3), several unknown parameter must be known in advance as well: AA^*, n, K, R_s and T temperature. In the following, we present a simple method to fit these parameters from several simple measurements using an auxiliary light source of unknown optical parameters instead of external electrical current generator or voltage source (e.g. a source-measurement unit).

Our aim is to circumvent equipment-based calibration forced current-voltage situation and precise temperature measurement. Thus, we propose the following model parameter identification method: .

- The measurement process is performed to record V_{OC} and I_{SC} point series at different illumination and temperature values as described in the next steps.
- A light source provides a broad range of illumination cases to the photodiode at a stable temperature in order to generate numerous voltage-current pairs.
- These sweeps are repeated for various temperature values (e.g. 20–100 C^o). The exact temperature values are not of importance, only stability during the sampling time.
- The missing parameters are fitted to the voltage-current pairs using the diode equations.

In the presented setup, the varying illumination was generated by an auxiliary laser diode that was driven with a current ramp from complete off-state to nominal output power (LED or blocked, modulated sunlight would be adequate as well). The reason for the additional laser in this setup is to avoid heating effect of the integrated laser diode during parameter fitting, thus this laser source is used solely during this step. The recorded V_{OC} and I_{SC} series are then fed into a constrained nonlinear multivariable cost function minimalization function (fmincon function of Matlab). The cost function of quadratic minimization is defined as follows: j, i are the indexes of the data pairs of i^{th} measurement point at the j^{th} stable ambient temperature.

$$I_{0,j} = AA^* T_j^K exp\left(-\frac{q\phi_B(T_j)}{nkT_j}\right) \tag{4}$$

$$\epsilon(j,i) = I_{SC}(j,i) - I_{0,j}\left(exp\left(\frac{q(V_{OC}(j,i) - I_{SC}(j,i)R_s)}{nkT_j}\right) - 1\right) + I_{bias} \tag{5}$$

$$F(V_{OC}, I_{SC}) = \sum_{\forall j}\sqrt{\sum_{\forall i}\frac{\epsilon(j,i)^2}{|I_{SC}(j,i)| + \Delta}} \tag{6}$$

Eqs. (4) and (5) are the error of the estimated and the measured diode current. Eq. (6) expresses the cost function as the summation of the error of each individual samples. The normalization factor $|I_{SC}(j, i)| + \Delta$ helps to weight the low photocurrent values during optimization. Δ is introduced to avoid near zero division ($\Delta = 1\mu A$). I_{bias} is an offset current added to I_{SC} to handle miscellaneous measurement and quantization errors.

3. Thermal simulation

First, to understand the behavior of the temperature dynamics of a TO package, we simulated a $5.6mm$ laser diode package with transient finite element method (COMSOL Multiphysics [24]). The model contained a case, a laser diode, a photodiode and the bond wires. The diode was placed in a $2 \times 2 \times 0.5cm^3$ sized copper heat sink with cylindrical hole, the diode was powered up with a constant heat flux of a typical $250mW$ optical output power ($\approx 0.6W$). The goal of this analysis was to compare the temporal and temperature dynamics of the heat sink, near the junction area and the photodiode temperature. Two configurations were simulated, namely a tight and an intentionally loose thermal connection between the package of the laser diode and the heat sink. In the latter configuration, only the electrical connections were maintained with an air gap between the heat sink surface and the socket. As it can be seen in Fig. 1, the laser heated up the most from its initial room temperature, and the photodiode and the heat sink followed its temperature rise with smaller amount and longer settling time.

4. Experiments

4.1. Measurement setup

The open circuit voltage and the short circuit current values cannot be measured at the same instant, thus a technique is needed to switch between the two cases. In the sensor readout circuit, shown in Fig. 2, we used two analog multiplexers with two distinct branches, namely a low noise transimpedance amplifier (TIA) [25–27] and a non-inverting voltage amplifier. The role of the TIA is to convert the photocurrent to voltage maintaining zero voltage on the photodiode terminals (zero bias mode). When a branch is disconnected from the photodiode, its input is

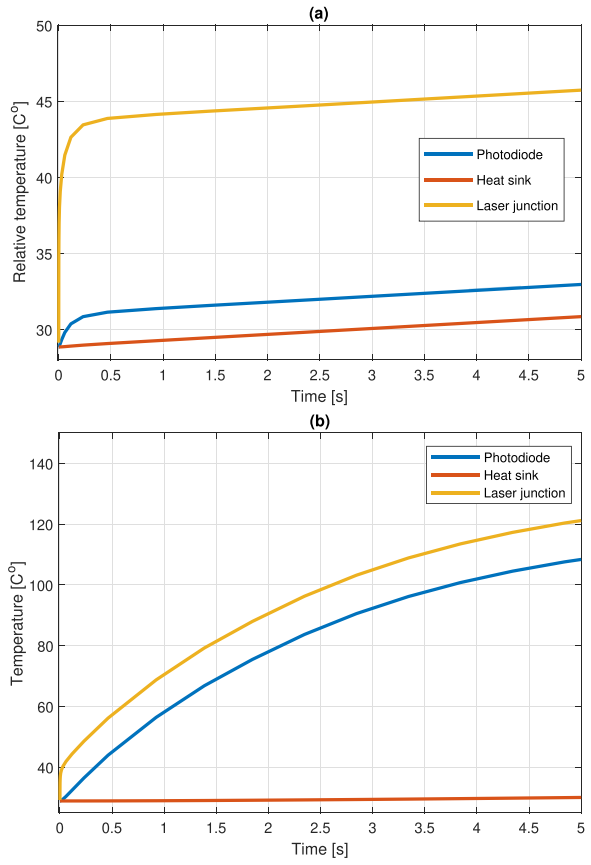

Fig. 1. Transient finite element simulation of a typical 5.6 mm laser diode case including monitor photodiode with 250mW output power transient: (a) tight thermal connection to the heat sink. (b) loose thermal connection to the heat sink.

connected to its corresponding zero level: the input of the TIA is disconnected and the voltage follower is connected to signal ground level. The two branches are simulatenously digitalized, hence in both multiplexer positions the offset error of one branch can be measured and then used for bias compensation (amplifier input bias voltage). The period time of the alternating measurements is limited by the settling time of the two cases. The settling time is dominated by the carrier diffusion time. The capacitance of the photodiode in zero bias configuration is significantly lower than in the open circuit case (the depletion region acts as the plates of a capacitor), thus this mode limits the alternating frequency. We can distinguish several noise sources, such as the Johnson noise from the load resistor, the shot noise from the incident light, and the instrumentation voltage and quantization noise. The photodiode related noise is suppressed by operating the photodiode in zero voltage or zero current modes [28] in both cases. The presented setup provided 14μV and 4.8nA RMS noise for voltage and current measurements (in the 0.1 Hz to a few kHz bandwidth).

We used the setup shown in Fig. 3 as a typical temperature-controlled laser scenario for demonstration. It is based on a laser diode mount with a thermoelectric-cooled mount (TEC, LDM21, Thorlabs Inc., USA), a TEC controller to monitor and set heat sink temperature (TED200C, Thorlabs Inc., USA) that uses an Analog Devices AD592 temperature sensor, and a current controller (LDC205C, Thorlabs Inc., USA) to drive the laser diode. The diode is an RLD82PZJ2 type of 820 nm central wavelength, 250mW optical output power (ROHM Co., Ltd., Japan). The auxiliary diode used for external illumination was a 645nm center wavelength 24mW output power laser diode (RLD63NPC8, ROHM Co., Ltd., Japan). The interfacing between the host computer and the auxiliary laser diode modulation, and the controlling of measurement type were done by a data acquisition card (USB-6211, National Instruments Co., Austin, TX, USA). The timing of the auxiliary laser beam was verified by a Si fixed gain detector (PDA015A/M, Thorlabs, Newton, NJ, USA), and a spectrometer (AvaSpec-ULS2048 StarLine, Avantes Ltd., The Netherlands) was used to estimate the laser junction temperature by its center wavelength shift at 1nm resolution. The room temperature central wavelength is measured by pulsed operation to avoid self-heating. The tested diode had $\approx 0.28nm/K$ wavelength shift. The beam of the auxiliary laser was directed to the measured laser diode in a tilted angle through a shortpass 805nm cutoff wavelength dichroic beamsplitter to avoid changing the characteristics of the main laser diode. The auxiliary laser was controlled by the data acquisition card during the parameter fitting process.

At low light level ($I_{SC} < 1\mu A$), the settling time is below 100μs allowing a corresponding few kHz modulation. We used a moderate 2

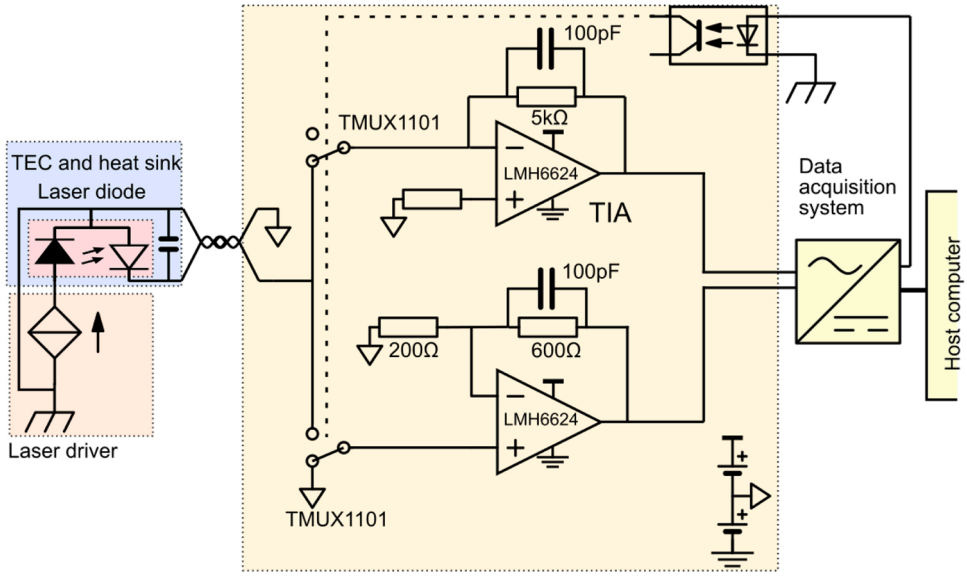

Fig. 2. Block diagram of the custom measurement board and connection to a representative laser diode case of *style A* pin arrangement. The monitor photodiode of the laser diode is connected to the measurement board, which switches to open circuit and short circuit measurement modes by a non-inverting and a transimpedance amplifier, respectively. The outputs are digitalized for processing.

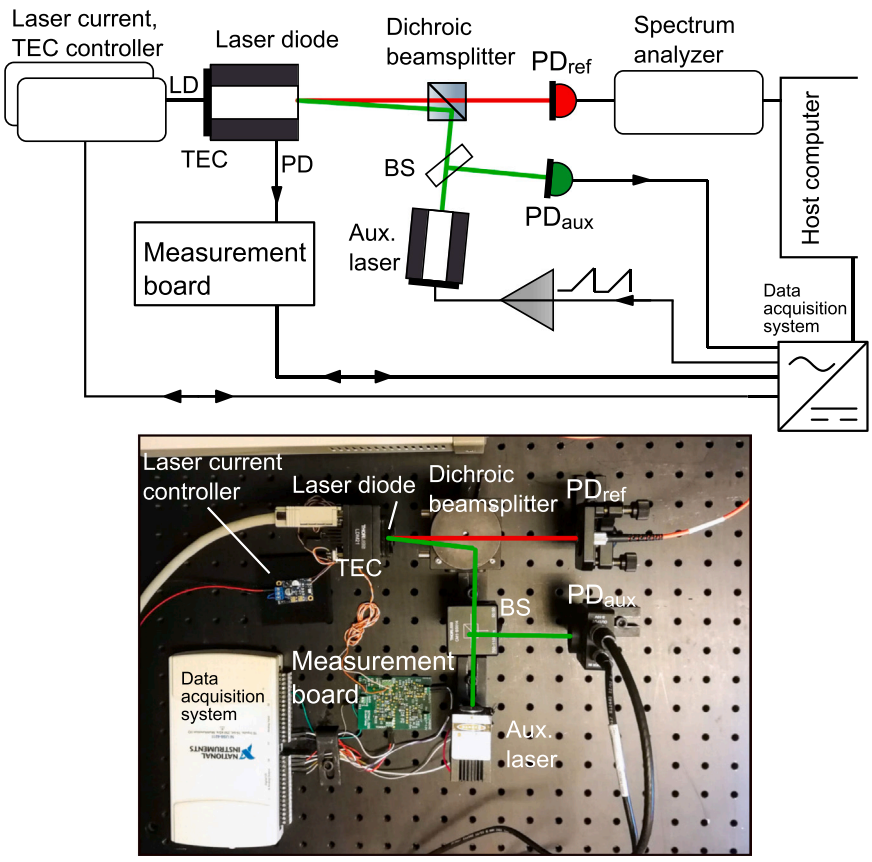

Fig. 3. Block diagram and a photo of the measurement system. The monitor photodiode of the laser diode is connected to the measurement board to alternate between measuring open circuit voltage and short circuit current. The controller monitors the temperature of the heat sink and operates the laser diode at constant current. The spectrum analyzer is used for observing the laser output quality and to measure the junction temperature based on its central wavelength. The auxiliary laser source provides a light input for calibration and model parameter fitting purposes.

KHz switching speed to achieve 1000 measurements per second with 2 V_{PP} range and 16-bit, 30.5μV resolution. A single measurement consisted of measuring each type of circuitry for 500μs with a 80kHz sampling rate resulting in 2 times 40 data points collected during the 1ms output period of a temperature estimate measurement. We first dropped the first epoch of the data removing the settling time and then replaced them with extrapolated ones calculated from the remaining data points. The results were then fed into the Eqs. (1)–(3) with the fitted constants to calculate the temperature. The ramp and data capture is repeated 25 times at five different ambient temperatures in the range of 15–50 C^o. The outcome of the fitting process can be seen in Fig. 4. In the example, the parameters became $AA^* = 21.36$, $n = 1.39$, $K = 1.42$, $I_{bias} = -16.2\mu A$, $R_s = 13\ \Omega$. These parameters are properties of the photodiodes, and so the same parameters apply to the device regardless of its location/usage specific conditions.

4.2. Measurements during operation

We first performed two steady state measurements at room temperature environment first without and then with the laser diode being in operation at its nominal output power. We waited for the temperature of the setup to stabilize, then recorded a time series for 5–5 min in both cases. The standard deviance was 3.8mK and 3.3mK of the photodiode temperature estimation for the dark and operational cases compared to the 2.8mK and 3.0mK standard deviance of the AD592 temperature sensor readings (see Fig. 5). Fig. 5c shows a histogram of the absolute temperature offset error of several repeated measurements at different temperatures and light levels (standard deviance was 0.49K with $\pm 3K$ limits). The measurement demonstrates that the light input (operational laser diode) does not decrease the precision and the absolute uncalibrated temperature offset remains in the range of the typical integrated silicon sensors.

Next, we present two transient measurements with good and loose thermal connection between the laser diode case and the heat sink similarly to the thermal simulation configurations. During the transients, no external illumination was provided. In the first experiment, the TEC temperature control was disabled, the laser diode was switched on ($t = 10s$) and then off ($t = 65s$), finally the heat sink thermal control is enabled again ($t = 150s$) to capture the effect of external heat flux to the case as shown in Fig. 6. The junction temperature was calculated from the central wavelength of the laser light while it was on with a limited resolution due to the limitation of the used spectrometer. In order to see the trend of the temperature change, beside the raw wavelength readings, shown as dots, a fitted curve is also included in the figures ?? a solid line. In the second experiment, we partially removed the laser diode to disconnect the heat sink and the package. We enabled the temperature control of the heat sink and waited for stable temperature readings. Then first the laser diode was switched on at $t = 1s$ and off at $t = 50s$. The measurement results can be seen in Figs. 7. The figure shows that the temperature of the photodiode rises quickly following the temperature of the poorly cooled laser diode. The two use cases illustrate that a photodiode can be used as temperature sensor with the proposed method regardless of the incoming light and with passive electrical measurements. Please note the similarity between the calculated and the simulated temperature behavior.

5. Discussion

If the laser light (or generally any external illumination) is negligible, then the open circuit voltage is dominant, as $I_{ph} \approx 0$, and this mode corresponds to other diode-based temperature sensor techniques [3]. If the laser is in operation, the strong effect of the photocurrent on the V_{OC} is compensated by the diode equations, providing an illumination independent temperature measurement method.

Repeated measurements of different arrangements and diodes resulted in absolute temperature differences, which remained in the

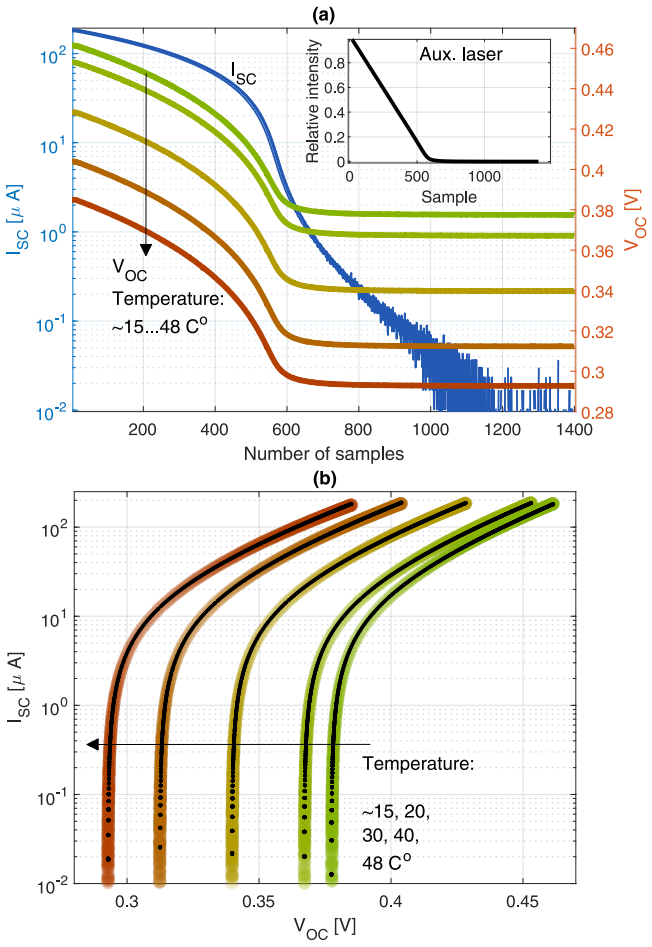

Fig. 4. The proposed parameter fitting uses a changing external optical stimuli, momentarily stabilized ambient temperature and the measurement of the zero biased photocurrent and open circuit voltage response of the photodiode. A decreasing current ramp drove the auxiliary laser that shone light onto the laser diode case at different temperatures. (a) shows the measured open circuit voltage and short circuit current at about 15, 20, 30, 40, 48 C^o ambient temperatures. The open circuit voltage curves are color coded from green to red scaled on the right axis. The short circuit current data is shown as overlapped blue curves scaled on the left axis). The inset shows the repeated relative light intensity of the auxiliary laser. (b) black dots are overlaid to show the outcome of the model calculation after substituting the fitted parameters. Both figures show 1400 by 25 samples at each temperature value.

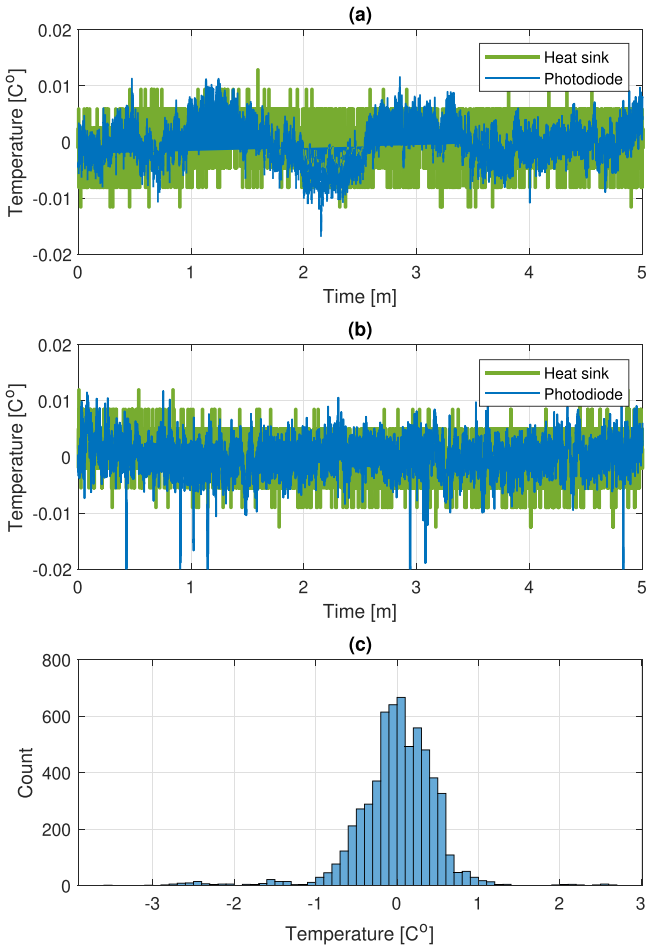

Fig. 5. Steady state temperature measurement stability comparison of the TEC-controlled heat sink temperature sensor and the photodiode. The measurement time was 5 min at 1 kHz sampling rate, the temperature offsets are removed for better visibility. The photodiode and the heat sink temperatures are plotted in the case of (a) no laser light, (b) with the laser diode operating at nominal optical output power (250 mW). The standard deviance of the temperature estimation for the dark and operational cases of the photodiode are 3.8mK and 3.3mK, the standard deviance of the heat sink temperature are 2.8mK and 3.0mK, respectively. (c) Absolute temperature offset error of repeated measurements of different static temperatures and diodes resulted (6000 samples, 15–48 C^o temperatures, changing light).

range of $\pm$ 3K. This offset value was compensated by single point calibration later on (see 5c). The presented calibration method for parameter fitting of the diode equation and several measurements showed us that, in some cases, there is a slight deviation in the range of $\pm$ 100mK in the temperature estimation at step-wise high light changes. The cause of the remaining illumination dependency may come from the simplified diode model, which could be extended with additional physical phenomena (e.g. ideality factor dependency, double diode model [11,29]), and from unresolved error sources of the measurement setup. Further constraints, such as parameters calculated with different measurement techniques [30] could further provide stability to the estimation process.

Besides this process, the photodiode can serve its original task while working as a temperature sensor, namely monitoring the emission of the laser diode (e.g. it can be used for automatic power control) with the short circuit current output. Furthermore, such a constant optical power control system could be extended to control the temperature of the laser diode as well with no additional sensor.

The presented setup could be significantly simplified by providing any reasonable, controllable external light source (e.g LED) directed to the photodiode for calibration and a variant of the I_{SC}, V_{OC} measurement board. Different laser diode case styles or pin arrangement can also be connected to such environment, preferably style B types with isolated photodiode connection. Other semiconductor devices can be temperature monitored similarly such as silicon, perovskite or organic solar cells [31,32], unamplified photodiode arrays, and organic photodetectors [33–36] in situations, where direct temperature sensor cannot be placed.

Author Agreement

All authors have seen and approved the final version of the manuscript being submitted. They warrant that the article is the authors' original work, hasn't received prior publication and isn't under consideration for publication elsewhere.

Declaration of Competing Interest

The authors declare that they have no known competing financial interests or personal relationships that could have appeared to influence

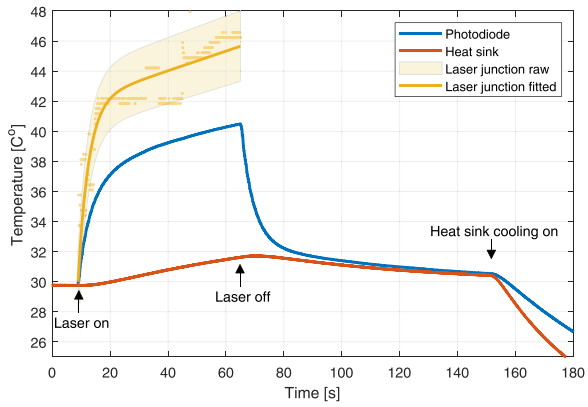

Fig. 6. Transient measurement with laser diode on/off period. The heat sink was monitored with a temperature sensor of the TEC controller, the photodiode temperature was calculated with the proposed technique from the open circuit voltage and short current alternating measurements. The laser junction temperature was derived from the central wavelength shift of the diode shown as dots and by a fitted curve.

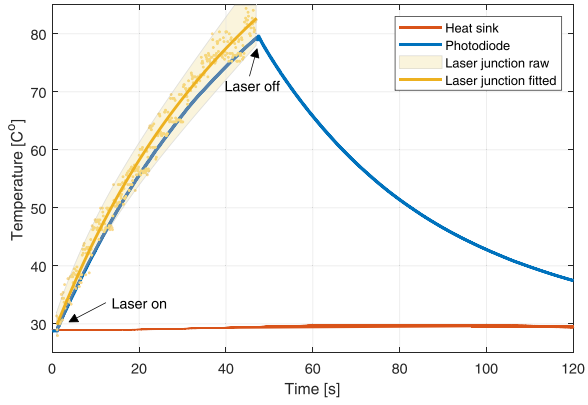

Fig. 7. Transient measurement with poor thermal connection between the case and the heat sink. The laser diode was first switched on then off.

the work reported in this paper.

References

[1] F. Reverter, X. Perpiñà, E. Barajas, J. León, M. Vellvehi, X. Jordà, J. Altet, Mosfet dynamic thermal sensor for ic testing applications, Sens. Actuators A:Phys. 242 (2016) 195–202.

[2] M. de Souza, M.A. Pavanello, D. Flandre, Low power highly linear temperaturesensor based on soi lateral pin diodes,in: 2016 IEEE SOI-3D-Subthreshold Microelectronics Technology Unified Conference (S3S), 2016: 1–3.

[3] M. Mansoor, I. Haneef, S. Akhtar, A. De Luca, F. Udrea, Silicon diodetemperature sensors-a review of applications, Sens. Actuators A:Phys. 232 (2015) 63–74.

[4] T. Dinh, H.-P. Phan, A. Qamar, P. Woodfield, N.-T. Nguyen, D.V. Dao, Thermoresistive effect for advanced thermal sensors: Fundamentals, Des., Appl., J. Micro Syst. 26 (5) (2017) 966–986.

[5] S. Rao, L. DiBenedetto, G. Pangallo, A. Rubino, S. Bellone, F. DellaCorte, 85-440 k temperature sensor based on a 4h-sic schottky diode, IEEE Sens. 16 (17) (2016) 6537–6542.

[6] S. Rao, G. Pangallo, F.G. DellaCorte, 4h-sic pin diode as highly lineartemperature sensor, IEEE Trans. Electron Devices 63 (1) (2015) 414–418.

[7] C.-P. Liu, H.-P. Huang, A cmos voltage reference with temperature sensor usingself-ptat current compensation, in:Proceedings 2005 IEEE International SOCConference, 2005: 37–42.

[8] H. Norde, A modified forward i-v plot for schottky diodes with high seriesresistance, J. Appl. Phys. 50 (7) (1979) 5052–5053.

[9] K. Sato, Y. Yasumura, Study of forward i-v plot for schottky diodes with highseries resistance, J. Appl. Phys. 58 (9) (1985) 3655–3657.

[10] S. Cheung, N. Cheung, Extraction of schottky diode parameters from forwardcurrent-voltage characteristics, Appl. Phys. Lett. 49 (2) (1986) 85–87.

[11] D.S. Chan, J.C. Phang, Analytical methods for the extraction of solar-cellsingle-and double-diode model parameters from iv characteristics, IEEE Trans. Electron Devices 34 (2) (1987) 286–293.

[12] V. Mikhelashvili, G. Eisenstein, R. Uzdin, Extraction of schottky diodeparameters with a bias dependent barrier height, Solid-State Electron. 45 (1) (2001) 143–148.

[13] E. Kowalczyk, L. Ornoch, Z. Gniazdowski, B. Mroziewicz, Dynamics ofthermo-optical properties of semiconductor lasers (International Society for Opticsand Photonics), High. -Power Diode Laser Appl. V. vol. 6456 (2007) 64561G.

[14] R. Puchert, A. Barwolff, M. Voß, U. Menzel, J.W. Tomm, J. Luft, Transient thermal behavior of high power diode laser arrays, IEEE Trans. Comp. Packag. Technol. 23 (1) (2000) 95–100.

[15] D. Iero, M. Merenda, R. Carotenuto, G. Pangallo, S. Rao, G. Brezeanu, F.G. D. Corte, A technique for improving the precision of the direct measurement ofjunction temperature in power light-emitting diodes, Sensors 21 (9) (2021) 3113.

[16] A. Kozlowska, Infrared imaging of semiconductor lasers, Semicond. Sci. Technol. 22 (8) (2007) R27.

[17] N.G. Usechak, J.L. Hostetler, Single-shot, high-speed, thermal-interfacecharacterization of semiconductor laser arrays, IEEE J. Quantum 45 (5) (2009) 531–541.

[18] C.-T. Sah, R.N. Noyce, W. Shockley, Carrier generation and recombination in pnjunctions and pn junction characteristics, Proceedings of the IRE 45 (9)(1957) 1228–1243.

[19] H. Card, E. Rhoderick, Studies of tunnel mos diodes i. interface effects insilicon schottky diodes, J. Phys. D: Appl. Phys. 4 (10) (1971) 1589.

[20] R. Tung, Electron transport at metal-semiconductor interfaces: General theory, Phys. Rev. B 45 (23) (1992) 13509.

[21] C.T. Dervos, P.D. Skafidas, J.A. Mergos, P. Vassiliou, pn junctionphotocurrent modelling evaluation under optical and electrical excitation, Sensors 4 (5) (2004) 58–70.

[22] T. Swe, K. Yeo, An accurate photodiode model for dc and high frequency spicecircuit simulation,in:Technical Proceedings of the 2001 InternationalConference on Modeling and Simulation of Microsystems, vol. 1, Citeseer, 2001, 362–365.

[23] I. Vainshtein, A. Zatsepin, V. Kortov, Applicability of the empirical varshnirelation for the temperature dependence of the width of the band gap, Phys. Solid State 41 (6) (1999) 905–908.

[24] COMSOL, Multiphysics version 5.6., Comsol Inc., MA, USA, 2020.

[25] N. Lockerbie, K. Tokmakov, A low-noise transimpedance amplifier for thedetection of “violin-mode"Ï resonances in advanced laser interferometergravitational wave observatory suspensions, Rev. Sci. Instrum. 85 (11) (2014), 114705.

[26] S. Zhang, C. Zhang, X. Pan, N. Song, High-performance fully differentialphotodiode amplifier for miniature fiber-optic gyroscopes, Opt. Express 27 (3) (2019) 2125–2141.

[27] A. Pullia, F. Zocca, Low-noise current preamplifier for photodiodes withdc-current rejector and precise intensity meter suited for optical lightspectroscopy, in:IEEE Nuclear Science Symposuim & Medical ImagingConference, IEEE, 2010, 1343–1345.

[28] Y. Wei, T. Lehmann, L. Silvestri, H. Wang, F. Ladouceur, Photodiode working inzero-mode: detecting light power change with dc rejection and acamplification, Opt. Express 29 (12) (2021) 18915–18931.

[29] S. Demirezen, Ş. Altíndal, I. Uslu, Two diodes model and illuminationeffect on the forward and reverse bias i-v and c-v characteristics ofau/pva (bi-doped)/n-si photodiode at room temperature, Curr. Appl. 13 (1) (2013) 53–59.

[30] R. Ocaya, F. Dejene, Estimating p-n diode bulk parameters, bandgap energy andabsolute zero by a simple experiment, Eur. J. Phys. 28 (1) (2006) 85.

[31] K. Emery, Measurement and characterization of solar cells and modules, Handb. Photovolt. Sci. Eng. 16 (2003) 701.

[32] W. Tress, K. Domanski, B. Carlsen, A. Agarwalla, E.A. Alharbi, M. Graetzel, A. Hagfeldt, Performance of perovskite solar cells under simulatedtemperature-illumination real-world operating conditions, Nat. Energy 4 (7) (2019) 568–574.

[33] H. Ren, J.-D. Chen, Y.-Q. Li, J.-X. Tang, Recent progress in organicphotodetectors and their applications, Adv. Sci. 8 (1) (2021), 2002418.

[34] Z. Wu, W. Yao, A.E. London, J.D. Azoulay, T.N. Ng, Temperature-dependentdetectivity of near-infrared organic bulk heterojunction photodiodes, ACS Appl. Mater. Interfaces 9 (2) (2017) 1654–1660.

[35] S. Züfle, N. Christ, S.W. Kettlitz, S. Valouch, U. Lemmer, Influence oftemperature-dependent mobilities on the nanosecond response of organic solarcells and photodetectors, Appl. Phys. Lett. 97 (6) (2010) 178.

[36] Z. Lan, Y. Lei, W.K.E. Chan, S. Chen, D. Luo, F. Zhu, Near-infrared andvisible light dual-mode organic photodetectors, Sci. Adv. 6 (5) (2020) eaaw8065.

Péter F˝oldesy received his Ph.D. in 2002 from the Budapest University of Technology and Economics, Hungary, on the topic of integrated circuit design for early vision chips. He gained his D.Sc. degree in 2019, awarded by the Hungarian Academy of Sciences, Hungary, for his contribution to sub-THz and mmwave sensory technology. From 1996 to the present, he is employed by the Institute for Computer Science and Control (SZTAKI), Budapest, Hungary, where he is a Research Fellow. Since 2007, he is also with a member of the Péter Pázmány Catholic University, Faculty of Information Technology and Bionics.

Imre Jánoki received his B.Sc. degree in Molecular Bionics Engineering and he is currently finishing his M.Sc. degree in Info-Bionics Engineering at the Faculty of Information Technology and Bionics of Péter Pázmány Catholic University. He works as an engineer at the Institute for Computer Science and Control (SZTAKI), Budapest, Hungary. His research interest is currently focused on the application of computer vision, physical sensors and machine learning in non-contact medical monitoring systems.

Ádám Nagy received his B.Sc. degree in Molecular Bionics Engineering and his M.Sc. degree in Info- Bionics Engineering from the Faculty of Information Technology and

Bionics of Péter Pázmány Catholic University. He is currently a Ph.D student at the Institute for Computer Science and Control, Budapest, Hungary. His research interests currently includes the application of computer vision, physical sensors and machine learning for solving medical problems.

Máté Siket received his B.Sc. degree in mechatronics and his M.Sc. degree in biomedical engineering from the Budapest University of Technology and Economics. He is currently pursuing a Ph.D. degree at Óbuda University and works as an engineer at the Institute for Computer Science and Control (SZTAKI). His current research interests include controlling and modeling of physiological systems and non-contact vital sign monitoring.

Ákos Zarándy received his Ph.D. and D.Sc. from the Hungarian Academy of Sciences in 1997 and in 2010 respectively, in electrical engineering and computer science. He is a research advisor at the Institute for Computer Science and Control (SZTAKI), Budapest, Hungary and also a professor at the Péter Pázmány Catholic University. His research interest is computer vision, physical sensors and image sensing with special sensors and optics.